

1 **Assessment of Sea Ice Simulations in the CMIP5**

2 **Models**

3
4 **Qi Shu^{1,2}, Zhenya Song^{1,2}, Fangli Qiao^{1,2}**

5 1 {First Institute of Oceanography, State Oceanic Administration, Qingdao 266061}

6 2 {Key Lab of Marine Science and Numerical Modeling, SOA, Qingdao 266061}

7 Correspondence to: Fangli Qiao (qiaofl@fio.org.cn)

8 9 **Abstract**

10 The historical simulations of sea ice during 1979 to 2005 by the Coupled Model
11 Intercomparison Project Phase 5 (CMIP5) are compared with satellite observations,
12 Global Ice-Ocean Modeling and Assimilation System (GIOMAS) output data and
13 Pan-Arctic Ice Ocean Modeling and Assimilation System (PIOMAS) output data in
14 this study. Forty-nine models, almost all of the CMIP5 climate models and Earth
15 System Models with historical simulation, are used. For the Antarctic, multi-model
16 ensemble mean (MME) results can give good climatology of sea ice extent (SIE), but
17 the linear trend is incorrect. The linear trend of satellite-observed Antarctic SIE is
18 $1.29(\pm 0.57) \times 10^5 \text{ km}^2 \text{ decade}^{-1}$; only about 1/7 CMIP5 models show increasing
19 trends, and the linear trend of CMIP5 MME is negative with the value of $-3.36(\pm 0.15)$
20 $\times 10^5 \text{ km}^2 \text{ decade}^{-1}$. For the Arctic, both climatology and linear trend are better
21 reproduced. Sea ice volume (SIV) is also evaluated in this study, and this is a first
22 attempt to evaluate the SIV in all CMIP5 models. Compared with the GIOMAS and
23 PIOMAS data, the SIV values in both Antarctic and Arctic are too small, especially
24 for the Antarctic in spring and winter. The GIOMAS Antarctic SIV in September is
25 $19.1 \times 10^3 \text{ km}^3$, while the corresponding Antarctic SIV of CMIP5 MME is 13.0×10^3
26 km^3 , almost 32% less. The Arctic SIV of CMIP5 in April is $27.1 \times 10^3 \text{ km}^3$, which is

27 also less than that from PIOMAS SIV ($29.5 \times 10^3 \text{ km}^3$). This means that the sea ice
28 thickness simulated in CMIP5 is too thin although the SIE is fairly well simulated.

29

30 **1. Introduction**

31 The Coupled Model Intercomparison Project Phase 5 (CMIP5) provides a very useful
32 platform for studying climate change. Simulations and projections by more than 60
33 state-of-the-art climate models and Earth System Models are archived under CMIP5.
34 Assessment of the performance of CMIP5 outputs is necessary for scientists to decide
35 which model outputs to use in their research and for model-developers to improve
36 their models. Here, we focus on the assessment of sea ice simulations under CMIP5
37 historical experiment. The CMIP5 data portal contains sea ice outputs from 49
38 coupled models. Many of these CMIP5 sea ice simulations have been evaluated and
39 several valuable studies have been published.

40 For the Antarctic, the main problem of the CMIP5 models is their inability to
41 reproduce the observed slight increase of sea ice extent (SIE). Turner et al. (2013) first
42 assessed CMIP5 Antarctic SIE simulations using 18 models, and summarized that the
43 majority of these models have too little SIE at the minimum sea ice period of
44 February, and the mean of these 18 models' SIE shows a decreasing trend over
45 1979-2005, opposite to the satellite observation that exhibits a slight increasing trend.
46 Polvani et al. (2013) used four CMIP5 models to study the cause of observed
47 Antarctic SIE increasing trend under the conditions of increasing greenhouse gases
48 and stratospheric ozone depletion. They concluded that it is difficult to attribute the
49 observed trend in total Antarctic sea ice to anthropogenic forcing. Zunz et al. (2013)
50 suggested that the model Antarctic sea ice internal variability is an important metric to
51 evaluate the observed positive SIE trend. Using simulations from 25 CMIP5 models,
52 Mahlstein et al. (2013) pointed that internal sea ice variability is large in the Antarctic
53 region and that both the observed and simulated trends may represent natural variation
54 along with external forcing.

55 For the Arctic, CMIP5 models offer much better simulations. Stroeve et al. (2012)
56 evaluated CMIP5 Arctic SIE trends using 20 CMIP5 models. They found that the
57 seasonal cycle of SIE was well represented, and that the simulated SIE decreasing
58 trend was more consistent with the observations over the satellite era than that of
59 CMIP3 models but still smaller than the observed. They also noted the spread in
60 projected SIE through the 21st century from CMIP5 models is similar to that from
61 CMIP3 models. Massonnet et al. (2012) examined 29 CMIP5 models, and provided
62 several important metrics to constrain the projections of summer Arctic sea ice
63 projection. Liu et al. (2013) also pointed out that CMIP5 projections have large
64 inter-model spread, but they also found that they could reproduce observed Arctic
65 ice-free time by reducing the large spread using two different approaches with 30
66 CMIP5 models.

67 These studies only used some of CMIP5 models' outputs because other CMIP5 model
68 outputs were not yet submitted. By now, all the CMIP5 participants have finished
69 their model runs and submitted their model outputs. So, here we will evaluate all
70 CMIP5 sea ice simulations, in an attempt to provide the community a useful
71 reference.

72 The rest of the paper is structured as follows. Section 2 presents sea ice data and
73 analysis methodology used in this study. Model assessment is given in section 3.
74 Conclusions and discussion are provided in section 4.

75

76 **2. Data and Methodology**

77 Sea ice simulations of CMIP5 historical runs from 49 CMIP5 coupled models are now
78 available. Monthly sea ice concentration (SIC) and sea ice thickness from these
79 models are used in this study. These outputs are published by the Earth System Grid
80 Federation (ESGF) (<http://pcmdi9.llnl.gov/esgf-web-fe/>) by each institute that is
81 responsible for its model. Although there are several ensemble realizations of each
82 CMIP5 model, the standard deviation between different ensemble realizations of each

83 model is small (Turner et al., 2013; Table 1). So, here we only choose the first
84 realization of each model for the analysis. CMIP5 historical runs cover the period
85 from 1850 to 2005, but the continuous sea ice satellite record only started in 1979; so
86 the period of 1979-2005 is chosen for the following analysis. Monthly
87 satellite-observed SIC is used in this study, which is based on the National
88 Aeronautics and Space Administration (NASA) team algorithm (Cavalieri et al., 1996)
89 provided by the National Snow and Ice Data Centre (NSIDC)
90 (<http://nsidc.org/data/seaice/>). Satellite observed sea ice extent used here is also from
91 NSIDC (<ftp://sidacs.colorado.edu/DATASETS/NOAA/G02135/>). Sea ice volume
92 (SIV) is an important index for assessment of sea ice simulation although direct
93 observations of SIV are very limited. SIV in the Antarctic used here is from the
94 Global Ice-Ocean Modeling and Assimilation System (GIOMAS)
95 (http://psc.apl.washington.edu/zhang/Global_seaice/index.html). SIV in the Arctic is
96 from Pan-Arctic Ice Ocean Modeling and Assimilation System (PIOMAS)
97 ([http://psc.apl.washington.edu/wordpress/research/projects/arctic-sea-ice-volume-ano-](http://psc.apl.washington.edu/wordpress/research/projects/arctic-sea-ice-volume-anomaly/)
98 [maly/](http://psc.apl.washington.edu/wordpress/research/projects/arctic-sea-ice-volume-anomaly/)). Note that SIV data from GIOMAS and PIOMAS are not observations but
99 model simulations with data assimilation. The climatology and linear trends of
100 CMIP5 simulated SIE, SIC and SIV are compared with satellite observations and
101 GIOMAS and PIOMAS data. CMIP5 simulated SIE is computed as the total area of
102 all grid cells where SIC exceeds 15%. SIV is computed as the sum of the product of
103 SIC, the area of grid cell and sea ice thickness of each grid cell. All gridded SIC and
104 sea ice thickness are re-gridded onto 1.0° longitude by 1.0° latitude grids before the
105 analysis is performed. In this study, spring is from March to May for the Arctic, and
106 from September to November for the Antarctic. Summer, autumn and winter are
107 defined accordingly.

108

109 **3. Results**

110 We select several metrics to assess the sea ice simulations in CMIP5 models. Mean
111 state, seasonal cycle, the model internal variability, linear trends and simulated errors

112 are used. For the Arctic sea ice, model mean state and seasonal cycle are important to
113 Arctic sea ice projection (Massonnet et al., 2012). For the Antarctic sea ice, the model
114 internal variability is an important metric to evaluate the observed positive SIE trend
115 (Zunz et al., 2013). Annual mean SIE, SIE amplitude, standard deviation of detrended
116 SIE anomaly (SIE variability), SIE linear trend and CMIP5 simulated SIE root mean
117 square (RMS) error are shown in Table 1 and Table 2. The same metrics for SIV are
118 also shown in Table 1 and Table 2. Each CMIP5 model simulated SIC and sea ice
119 thickness are given in the Supplementary. Detailed analyses for Antarctic and Arctic
120 are as follows.

121

122 **3.1 Assessment of Antarctic sea ice simulations**

123 CMIP5 multi-model ensemble mean (MME) Antarctic climatological SIE compares
124 well with the satellite-observed SIE, but the inter-model spread is large (Fig. 1a and
125 Table 1). Satellite observations show that the Antarctic SIE has the minimum value of
126 3.0 million km² in February and the maximum value of 18.7 million km² in
127 September, and the annual mean SIE is 11.94 million km². CMIP5 MME SIE has the
128 minimum and maximum values of 3.3 and 18.7 million km², and annual mean SIE of
129 11.50 million km², respectively. The seasonal cycle of observed SIE is well
130 represented by the MME SIE of the 49 CMIP5 coupled models. Satellite observed
131 monthly SIE amplitude is 15.70 million km², and CMIP5 MME value is 15.46 million
132 km². The simulated SIE errors are very small for each month. The simulated SIE
133 errors are smaller than 15% of the observations, except for March and April SIE
134 values, which are a little less than 85% of the observations. One standard deviation of
135 CMIP5 simulations, which is larger than 15% of the observations (Fig. 1a), show that
136 CMIP5 coupled models have large spread each month in terms of Antarctic SIE. Table
137 1 also shows that CMIP5 models have large spread. BNU-ESM has the largest annual
138 mean and amplitude of SIE with the values of 20.60 and 23.46 million km², and
139 MIROC5 has the smallest annual mean and amplitude of SIE with the values of 3.23

140 and 6.62 million km² (highlighted in Table 1 with bold font), respectively. BNU-ESM
141 simulated February SIE is even larger than MIROC5 simulated September SIE. Large
142 SIE spread and small MME SIE errors indicate that we should use as many models as
143 we can when using CMIP5 outputs.

144 CMIP5 model simulated and satellite observed SICs in February and September
145 during 1979-2005 are shown in Supplementary Figures 1 and 2. In February most
146 models have too less SIC compared with satellite observed, especially in the
147 Bellingshausen Sea and the Amundsen Sea. More than half of CMIP5 models have no
148 sea ice in the Bellingshausen Sea and the Amundsen Sea. CNRM-CM5,
149 GFDL-CM2p1, GFDL-CM3, GFDL-ESM2G, GFDL-ESM2M, IPSL-CM5B-LR and
150 MIROC5 almost have no sea ice in February in the Antarctic. But ACCESS1.3,
151 BNU-ESM, CCSM4, CESM1-BGC, CESM1-FASTCHEM, CSIRO-Mk3.6,
152 FGOALS-g2, FIO-ESM and NorESM1-ME have more sea ice than satellite
153 observations. Although CMIP5 simulated MME SIE fits the observations well, MME
154 spatial map of SIC fits the observations not so well. MME SICs in the Weddell Sea,
155 the Bellingshausen Sea and the Amundsen Sea are too little. In September, most
156 CMIP5 models have better performance than that in February, and MME SIC also has
157 better spatial pattern.

158 Figures 1b and 2 show that linear trends of CMIP5 MME Antarctic SIE do not agree
159 with the satellite observations. Many studies showed that Antarctic SIE has an
160 increasing trend since the end of 1970s (Cavalieri et al., 1997; Zwally et al., 2002;
161 Cavalieri et al., 2003; Turner et al., 2009). Satellite-observed Antarctic SIE has a
162 small increasing linear trend with the rate of $1.29(\pm 0.57) \times 10^5 \text{ km}^2 \text{ decade}^{-1}$ during
163 1979-2005, while CMIP5-simulated linear trend is $-3.36(\pm 0.15) \times 10^5 \text{ km}^2 \text{ decade}^{-1}$
164 (Fig. 1b). Only eight out of 49 CMIP5 models have increasing linear trends as the
165 observations (highlighted in Table 1 with bold font). They are BCC-CSM1.1,
166 CMCC-CESM, CNRM-CM5-2, GISS-E2-R-CC, IPSL-CM5A-MR, IPSL-CM5B-LR,
167 MPI-ESM-MR and MRI-CGCM3. This supports the conclusion by Polvani et al.
168 (2013) that it is difficult to attribute the observed Antarctic SIE trends to

169 anthropogenic forcing. From Table 1 we can see that several models (highlighted in
170 Table 1 with bold font) such as BCC-CSM1.1, BCC-CSM1-1-M, CanESM2,
171 CMCC-CESM, CNRM-CM5-2 and GISS-E2-R have large internal variabilities, and
172 these models always have large linear trends. This mean that the satellite observed
173 positive SIE trend may represent natural variation along with external forcing
174 (Mahlstein et al., 2013). Figure 2 shows that the monthly and seasonal trends of
175 CMIP5-simulated Antarctic SIE also do not agree with the observations. Observed
176 Antarctic SIE shows increasing trends in each month and each season, and the largest
177 trend is in March and the autumn season. CMIP5 MME SIE, however, has decreasing
178 trends in each month and each season, and the largest trend is in February and the
179 summer season.

180 The trends of observed Antarctic SIC have large spatial differences (Fig. 3), but the
181 simulated Antarctic SIC trends are almost decreasing everywhere (Fig. 4). Figure 3
182 shows that decreasing SIC is mainly in the Antarctic Peninsula, which is one of the
183 three high-latitude areas showing rapid regional warming over the last 50 years
184 (Vaughan et al., 2003). SIC also decreases in the Bellingshausen Sea and the
185 Amundsen Sea in summer and autumn. The increasing SIC is mainly in the Ross Sea
186 all year round and in the Weddell Sea in summer and autumn. Figure 4 clearly shows
187 that CMIP5 MME SIC has decreasing trend everywhere except in the coast of the
188 Amundsen Sea and in part of the Ross Sea in spring and winter.

189 SIV depends on both sea ice coverage and sea ice thickness. SIV is more directly tied
190 to climate forcing than SIE. So, SIV is an important climate indicator in climate study.
191 The observed sea ice thickness records are mainly from submarine, aircraft and
192 satellite. But the observations are not continuously spatially or temporally over a long
193 period (Stroeve et al., 2014). For the Antarctic, the observed sea ice thickness data are
194 more limited. A climatological $2.5^{\circ} \times 5.0^{\circ}$ gridded Antarctic sea ice thickness map
195 was provided until 2008 (Worby et al., 2008). Recently, there are several studies using
196 satellite observations of sea ice thickness (Kurtz and Markus, 2012; Xie et al., 2013).
197 These observations provide modelers with useful validation of their models. But,

198 these data are not easily used to long-term simulation validations by now because
199 these data are not too long enough. Here, we use GIOMAS data, which is from a
200 global ice-ocean model (Zhang and Rothrock, 2003) with data assimilation capability.
201 What we should keep in mind is that GIOMAS sea ice thickness is not from
202 observations and may also have large uncertainty. CMIP5-simulated and GIOMAS
203 Antarctic sea ice thicknesses during 1979-2005 are shown in Supplementary Figure 3.
204 GIOMAS outputs show that thick sea ice is mainly in the coasts of the Weddell Sea,
205 the Bellingshausen Sea and the Amundsen Sea. CMIP5 MME sea ice thickness can
206 give similar spatial patterns, but most of CMIP5 MME sea ice thickness is thinner
207 than GIOMAS sea ice thickness. The spatial pattern for each CMIP5 model has large
208 difference. BCC-CSM1.1, CESM1-CAM5-1-FV2, CMCC-CM, and CMCC-CMS fit
209 GIOMAS sea ice thickness well. Several CMIP5 models such as CCSM4,
210 CESM1-BGC, CESM1-FASTCHEM, FGOALS-g2 and FIO-ESM have too thick sea
211 ice near the coasts of the Antarctic.

212 CMIP5 SIV simulations have more problems than the SIE simulations. The main
213 problems of CMIP5 Antarctic SIV simulations include too big SIV in summer, too
214 small SIV in winter, too large model spread, and wrong linear trend compared with
215 the GIOMAS data (Fig. 5). The annual mean SIV from GIOMAS is $11.02 \times 10^3 \text{ km}^3$,
216 but CMIP5 MME SIV is only $7.73 \times 10^3 \text{ km}^3$ (Table 1). In February, Antarctic SIV
217 from GIOMAS is $1.9 \times 10^3 \text{ km}^3$, while the CMIP5 MME is $2.7 \times 10^3 \text{ km}^3$. In
218 September, GIOMAS SIV is $19.1 \times 10^3 \text{ km}^3$, while CMIP5 MME is only 13.0×10^3
219 km^3 , almost 32% less than the GIOMAS. We can also see from Figure 5a that the
220 model spread of Antarctic SIV in CMIP5 is very large. The one standard deviation of
221 modeled SIV is much larger than 15% of the GIOMAS data in every month. We
222 checked the correlation between SIE RMS error and SIV RMS error, and we can find
223 that the models with small SIE RMS errors always have small SIV RMS errors (Table
224 1). It means that for the Antarctic models with a more realistic SIE mean state may
225 result in a convergence of estimates of SIV. Figure 5b shows that GIOMAS SIV has
226 an increasing trend of $0.45(\pm 0.09) \times 10^3 \text{ km}^3 \text{ decade}^{-1}$, while CMIP5 MME SIV has a

227 decreasing trend of $-0.36(\pm 0.01) \times 10^3 \text{ km}^3 \text{ decade}^{-1}$. If we check each CMIP5 model
228 separately, we will also find only eight out of the 49 CMIP5 models have increasing
229 SIV trend that is consistent with the GIOMAS. They are BCC-CSM1.1,
230 CMCC-CESM, CNRM-CM5-2, IPSL-CM5A-MR, IPSL-CM5B-LR, MPI-ESM-MR,
231 MPI-ESM-P and MRI-CGCM3 (highlighted in Table 1 with bold font).

232

233 **3.2 Assessment of Arctic sea ice simulations**

234 CMIP5 shows a quite good annual cycle of Arctic SIE, but the model error in winter
235 is larger than that in summer and model spread is large (Fig. 6a). Arctic SIE reaches
236 the maximum value of 15.7 million km^2 in March, and reaches the minimum value of
237 6.9 million km^2 in September, and the annual mean value is 12.02 million km^2 . The
238 MME climatological SIE compares well with the satellite-observed SIE. CMIP5
239 MME SIE reaches the maximum value of 17.2 million km^2 , and reaches the minimum
240 value of 6.8 million km^2 , and the annual mean value is 12.81 million km^2 . The
241 modeled error is less than 15% of the observations in every month. CMIP5 MME SIE
242 is bigger than the satellite observation in spring, and the modeled error is quite small
243 at other times. The model spread is large, with one standard deviation of CMIP5
244 models bigger than 15% of the observed SIE in every month (Fig. 6a). CSIRO-MK3.6,
245 GFDL-ESM2G, GISS-E2-R-CC and MRI-CGCM3 have large annual mean SIE with
246 the values larger than 15 million square kilometers (highlighted in Table 2 with bold
247 font). CSIRO-MK3.6 has more sea ice in the Barents Sea in summer (Supplementary
248 Fig. 4). GFDL-ESM2G, GISS-E2-R-CC and MRI-CGCM3 have more sea ice in
249 winter (Supplementary Fig. 5). MIROC4h, MIROC-ESM, MIROC-ESM-CHEM and
250 MPI-ESM-P have small annual mean SIE with the values less than 11 million square
251 kilometers (highlighted in Table 1 with bold font). Arctic SIE amplitudes from CMIP5
252 models also have large spread. GISS-E2-R-CC has the largest amplitude with the
253 value of 16.73 million km^2 , and FGOAL-g2 has the smallest amplitude with the value
254 of only 3.35 million km^2 (highlighted in Table 2 with bold font). Compared with

255 Antarctic, CMIP5 simulated Arctic SIE variability has small spread (Column c in
256 Table 2).

257 CMIP5 MME SIE shows a decreasing trend that is consistent with the satellite
258 observation, though the decreasing rate is a little smaller than that of the observation
259 (Figs. 6b and 7). The satellite-observed SIE linear trend over the period of 1979-2005
260 is $-4.35(\pm 0.41) \times 10^5 \text{ km}^2 \text{ decade}^{-1}$, while CMIP5 MME SIE linear trend is only
261 $-3.71(\pm 0.19) \times 10^5 \text{ km}^2 \text{ decade}^{-1}$. BCC-CSM1.1 has the largest trend of $-8.79(\pm 0.97)$
262 $\times 10^5 \text{ km}^2 \text{ decade}^{-1}$. Thirty-one out of the 49 CMIP5 models have smaller decreasing
263 rate than the observation, and NorESM1-ME has the smallest trend of $-0.21(\pm 0.43)$
264 $\times 10^5 \text{ km}^2 \text{ decade}^{-1}$. Both observed and CMIP5-simulated SIE in autumn has the
265 largest decreasing trend. CMIP5-simulated difference of SIE decreasing trend
266 between summer and autumn is, however, larger than that of the observations. The
267 main reason is CMIP5-simulated SIE has small reduction in summer, especially in
268 July (Fig. 7). Satellite-observed SIE decreasing rate is 5.22% per decade in July, while
269 the CMIP5-simulated decreasing rate is 3.54% per decade. The largest decreasing rate
270 is in September; the observed trend is -8.61% per decade and the simulated trend is
271 -8.46% per decade.

272 Figure 8 and 9 show that the spatial patterns of CMIP5-simulated SIC reduction rate
273 are consistent with the observations from 1979 to 2005, but the decreasing rates are
274 smaller than the observed. In spring and winter, the observed decreasing SIC is
275 mainly in the Okhotsk Sea, Baffin Bay, Greenland Sea and Barents Sea;
276 CMIP5-simulated decreasing SIC is also in these regions. In summer and autumn, the
277 main decreasing SIC is in the Chukchi Sea, Barents Sea and Kara Sea (Figs. 8 and 9),
278 and CMIP5 MME SIC has similar characteristics. However, CMIP5 simulations have
279 larger trends in the central Arctic Ocean.

280 Stroeve et al. (2014) compared observed sea ice thickness data in the Arctic with that
281 of PIOMAS, and concluded that PIOMAS provides useful estimates of Arctic sea ice
282 thickness and SIV, and can be used to assess the CMIP5 models' performances.
283 Compared with PIOMAS sea ice thickness, the main problem of CMIP5 simulations

284 is too little Arctic SIV all year round and too large model spread (Fig. 10). In spring,
285 the Arctic has the largest SIV. Long-term mean PIOMAS SIV is maximum in April
286 with $29.5 \times 10^3 \text{ km}^3$, and the corresponding CMIP5 MME is $27.1 \times 10^3 \text{ km}^3$.
287 Long-term mean PIOMAS SIV is minimum in September with $13.3 \times 10^3 \text{ km}^3$, and
288 the corresponding CMIP5 MME is $9.6 \times 10^3 \text{ km}^3$. Amplitude of SIV from PIOMAS is
289 $16.17 \times 10^3 \text{ km}^3$, and CMIP5 MME can give good amplitude of SIV with 17.50×10^3
290 km^3 . CMIP5 SIV model spread is also very large: one standard deviation for each
291 month is much larger than 15% of GIOMAS SIV. CanESM2 has the smallest SIV of
292 $9.97 \times 10^3 \text{ km}^3$, and CMCC-CM has the largest SIV of $33.01 \times 10^3 \text{ km}^3$.
293 Supplementary Figure 6 shows that BCC-CSM1-1-M, CanCM4, CanESM2,
294 GFDL-CM2p1, GISS-E2-H, GISS-E2-H-CC, GISS-E2-R, GISS-E2-R-CC,
295 MIROC4h, MIROC-ESM, and MIROC-ESM-CHEM simulated sea ice thickness is
296 significantly undervalued. Sea ice thickness in CESM1-WACCM, CMCC-CESM,
297 CMCC-CM, FGOALS-g2, IPSL-CM5B-LR, NorESM1-M, NorESM1-ME is
298 significantly overvalued. Based on PIOMAS, the linear trend of Arctic SIV during
299 1979-2005 is $-2.14(\pm 0.14) \times 10^3 \text{ km}^3 \text{ decade}^{-1}$. CMIP5 MME trend has the same sign
300 but smaller value, at $-1.45(\pm 0.05) \times 10^3 \text{ km}^3 \text{ decade}^{-1}$. Unlike most of CMIP5 models,
301 CESM1-WACCM SIV has a slight positive trend during 1979-2005. The reason may
302 be CESM1-WACCM SIV has large variability ($2.07 \times 10^3 \text{ km}^3$), and its internal
303 variability is not in phase with the natural observed variability.

304

305 **4. Conclusions and discussion**

306 The first ensemble realizations of the 49 CMIP5 historical simulations are evaluated,
307 in terms of the performance of sea ice. Most CMIP5 models have several ensemble
308 realizations for historical simulations. Is the standard deviation of spatial patterns
309 between different ensemble realizations of each model is small? We plot the spatial
310 patterns of SIC in February (Supplementary Fig. 7) and September (Supplementary
311 Fig. 8) from different ensemble realizations from GISS-E2-R which has 15 ensemble
312 realizations and have more ensemble realizations than most CMIP5 models. We can

313 see that the standard deviation between different ensemble realizations from the same
314 model is comparable. So the first ensemble realization of each model should be able
315 to represent the model's performance.

316 Our results show that the Arctic sea ice simulations are better than the Antarctic sea
317 ice simulations, and SIE simulations are better than SIV simulations. CMIP5 MME
318 SIV is too less in winter and spring because the sea ice thickness in CMIP5 models is
319 too thin in winter and spring compared with the GIOMAS and PIOMAS data. In the
320 Antarctic, MME can reproduce good mean state and monthly amplitude for SIE, but
321 for SIV MME mean state and amplitude are smaller. In the Arctic, MME can
322 reproduce good mean state and monthly amplitude for both SIE and SIV. CMIP5
323 simulations have very different variability (indicated by standard deviation of
324 detrended monthly SIE and SIV) for different models. From Tables 1 and 2 we can
325 conclude that the performance of each model is different. For the Antarctic,
326 ACCESS1.0, BCC-CSM1.1, CESM1-CAM5-1-FV2, CMCC-CM, EC-EARTH,
327 GISS-E2-H-CC, MIROC-ESM, MIROC-ESM-CHEM, MRI-CGCM3, MRI-ESM1
328 and NorESM1-M can give better SIE and SIV mean state. For the Arctic, ACCESS1.3,
329 CCSM4, CESM1-BGC, CESM1-CAM5, CESM1-CAM5-1-FV2,
330 CESM1-FASTCHEM, EC-EARTH, MIROC5, NorESM1-M and NorESM1-ME can
331 give better mean state of SIE and SIV. The Arctic SIE linear trends of BNU-ESM,
332 CanCM4, CESM1-FASTCHEM, EC-EARTH, GFDL-CM2p1, HadCM3,
333 HadGEM2-AO, MIROC-ESM-CHEM, MPI-ESM-MR and MRI-ESM1 are closed to
334 the observations.

335 Both satellite-observed Antarctic SIE and GIOMAS Antarctic SIV show increasing
336 trends over the period of 1979-2005, but CMIP5 MME Antarctic SIE and SIV have
337 decreasing trends. Only eight models' SIE and eight models' SIV show increasing
338 trends. Can these few CMIP5 models give correct Antarctic sea ice trend? If we use
339 these eight CMIP5 models to plot Antarctic SIC trends (not shown) as in Fig. 4, we
340 will find that these eight CMIP5 model mean SIC trends have different spatial
341 patterns with the observations (Fig. 3) although their model mean SIE and SIV have

342 increasing trends. Satellite observed Antarctic SIE has increased trends, but when we
343 use satellite observed sea ice record, we should also keep in mind that satellite
344 observed sea ice record may also has large uncertainty. Eisenman et al. (2014) point
345 out that sensor transition may cause a substantial change in the long-term trend.

346 We can see that the CMIP5 MME does a good job in terms of climatological mean,
347 but their inter-model spread is large. The number of models used in published studies
348 is usually less than the total CMIP5 models. How many models can give similar good
349 simulations as all the available CMIP5 models? We first choose the CMIP5 models
350 randomly. The model number changes from 1 to 49. We then calculate the SIE and
351 SIV RMS errors between MME and observations or GIOMAS and PIOMAS datasets.
352 For each fixed model number, we choose these models randomly many times, and
353 then calculate the mean of the RMS errors. Figure 11 shows the ratio of SIE and SIV
354 RMS errors between the errors calculated using different number of CMIP5 models
355 and the errors calculated using all 49 CMIP5 models. We can see that the model errors
356 decrease quickly as the model number increases; and the more models we use, the
357 smaller error we have. For a fixed model number, the ratios of SIE are larger than the
358 ratios of SIV, and Antarctic SIE has the largest ratio. When the model number is
359 greater than 30, the model errors do not change much anymore. If we choose a
360 criterion of RMS error larger than 15% of all the model RMS error, the model number
361 of 22 is the critical number for Arctic SIE. It means that more than 22 CMIP5 models
362 should give similar MME as all 49 CMIP5 models.

363 In this study, satellite observations, PIOMAS and GIOMAS data during the period of
364 1979-2005 are used to access the sea ice simulations from CMIP5 models. We always
365 expect the models can capture the observed trends during this period. But we should
366 note that simulations without data assimilation are always out of phase with the
367 natural variability seen in the observations. So the differences between simulations
368 and observations can either be due to model biases or natural climate variability
369 (Stroeve et al., 2014).

370

371 **Acknowledgments**

372 Satellite-observed sea ice concentration data are provided by
373 <http://nsidc.org/data/seaice/>, sea ice extent are from
374 <ftp://sidads.colorado.edu/DATASETS/NOAA/G02135/>, GIOMAS sea ice data are
375 downloaded from http://psc.apl.washington.edu/zhang/Global_seaice/index.html, and
376 PIOMAS sea ice data are from
377 <http://psc.apl.washington.edu/wordpress/research/projects/arctic-sea-ice-volume-anomaly/>.
378 CMIP5 sea ice simulations are downloaded from
379 <http://pcmdi9.llnl.gov/esgf-web-fe/>. The authors thank the above data providers. This
380 work is supported by the National Basic Research Program of China (973 Program)
381 under Grant 2010CB950500, National Natural Science
382 Foundation of China(Grant no. 41306206), and the Project of Comprehensive
383 Evaluation of Polar Areas on Global and Regional Climate Changes
384 (CHINARE2014-04-04, CHINARE2014-04-01, and CHINARE2014-01-01).

385 **References**

386 Cavalieri, D. J., Parkinson, C. L., Gloersen, P., and Zwally, H.: Sea Ice Concentrations
387 from Nimbus-7 SMMR and DMSP SSM/I-SSMIS Passive Microwave Data, Boulder,
388 Colorado USA: NASA DAAC at the National Snow and Ice Data Center, 1996.

389 Cavalieri, D. J., Gloersen, P., Parkinson, C. L., Comiso, J. C., and Zwally, H. J.:
390 Observed hemispheric asymmetry in global sea ice changes, *Science*, 278(5340),
391 1104-1106, 1997.

392 Cavalieri, D. J., Parkinson, C. L., and Vinnikov, K. Y: 30-Year satellite record reveals
393 contrasting Arctic and Antarctic decadal sea ice variability, *Geophysical Research*
394 *Letters*, 30, 1970, doi:10.1029/2003GL018031, 2003.

395 Eisenman, I., Meier, W. N., and Norris, J. R.: A spurious jump in the satellite record:
396 has Antarctic sea ice expansion been overestimated?, *The Cryosphere*, 8, 1289-1296,
397 doi:10.5194/tc-8-1289-2014, 2014.

398 Kurtz, N., and Markus T.: Satellite observations of Antarctic sea ice thickness and
399 volume, *Journal of Geophysical Research*, 117, doi:10.1029/2012JC008141, 2012.

400 Liu, J., Song, M., Horton, R. M., and Hu, Y.: Reducing spread in climate model
401 projections of a September ice-free Arctic, *Proceedings of the National Academy of*
402 *Sciences*, 110(31), 12571-12576 , 2013.

403 Mahlstein, I., Gent, P. R., and Solomon, S.: Historical Antarctic mean sea ice area, sea
404 ice trends, and winds in CMIP5 simulations, *Journal of Geophysical Research:*
405 *Atmospheres*, 118(11), 5105-5110, 2013.

406 Massonnet, F., Fichefet, T., Goosse, H., Bitz, C. M., Philippon-Berthier, G., Holland,
407 M. M., and Barriat, P.-Y.: Constraining projections of summer Arctic sea ice, *The*
408 *Cryosphere*, 6, 1383-1394, doi:10.5194/tc-6-1383-2012, 2012.

409 Polvani, L. M., and Smith, K. L.: Can natural variability explain observed Antarctic
410 sea ice trends? New modeling evidence from CMIP5, *Geophysical Research Letters*,
411 40(12), 3195-3199, 2013.

412 Stroeve, J. C., Barrett, A., Serreze, M., and Schweiger, A.: Using records from
413 submarine, aircraft and satellite to evaluate climate model simulations of Arctic sea
414 ice thickness, *The Cryosphere Discussions*, 8, 2179–2212, 2014.

415 Stroeve, J. C., Kattsov, V., Barrett, A., Serreze, M., Pavlova, T., Holland, M., and
416 Meier, W. N.: Trends in Arctic sea ice extent from CMIP5, CMIP3 and observations,
417 *Geophysical Research Letters*, 39, L16502, doi:10.1029/2012GL052676, 2012.

418 Turner, J., Comiso, C., Marshall, G. J., Lachlan-Cope, T. A., Bracegirdle, T., Maksym,
419 T., Meredith, M. P., Wang, Z., and Orr, A.: Non-annular atmospheric circulation
420 change induced by stratospheric ozone depletion and its role in the recent increase of
421 Antarctic sea ice extent, *Geophysical Research Letters*, 36, L08502,
422 doi:10.1029/2009GL037524, 2009.

423 Turner, J., Bracegirdle, T. J., Phillips, T., Marshall, G. J., and Hosking, J. S.: An Initial
424 Assessment of Antarctic Sea Ice Extent in the CMIP5 Models, *Journal of Climate*, 26,
425 1473–1484, doi: <http://dx.doi.org/10.1175/JCLI-D-12-00068.1>, 2013.

426 Vaughan, D. G., Marshall, G. J., Connolley, W. M., Parkinson, C., Mulvaney, R.,
427 Hodgson, D. A., King, J. C., Pudsey, C. J., and Turner, J.: Recent rapid regional
428 climate warming on the Antarctic Peninsula, *Climatic Change*, 60(3), 243-274, 2003.

429 Worby, A. P., Geiger, C. A., Paget, M. J., Van Woert, M. L., Ackley, S. F., and
430 DeLiberty, T. L.: Thickness distribution of Antarctic sea ice, *Journal of Geophysical*
431 *Research: Oceans*, 113, C05S92, doi:10.1029/2007JC004254, 2008.

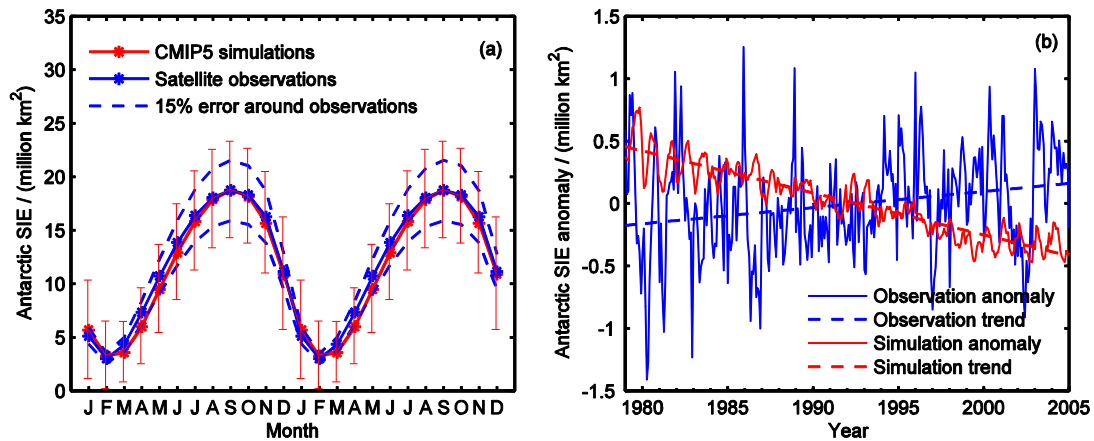
432 Xie, H., Tekeli, A. E., Ackley, S. F., Yi, D., and Zwally, H. J.: Sea ice thickness
433 estimations from ICESat altimetry over the Bellingshausen and Amundsen Seas,
434 2003–2009, *Journal of Geophysical Research: Oceans*, 118(5), 2438-2453, 2013.

435 Zhang, J., and Rothrock, D.: Modeling global sea ice with a thickness and enthalpy
436 distribution model in generalized curvilinear coordinates, *Monthly Weather Review*,
437 131, 845–861, 2003.

438 Zunz, V., Goosse, H., and Massonnet, F.: How does internal variability influence the
439 ability of CMIP5 models to reproduce the recent trend in Southern Ocean sea ice
440 extent?, *The Cryosphere*, 7, 451-468, doi:10.5194/tc-7-451-2013, 2013.

441 Zwally, H. J., Comiso, J. C., Parkinson, C. L., Cavalieri, D. J., and Gloersen, P.:
442 Variability of Antarctic sea ice 1979–1998, *Journal of Geophysical Research: Oceans*,
443 107(C5), 9-1-9-19, 2002.

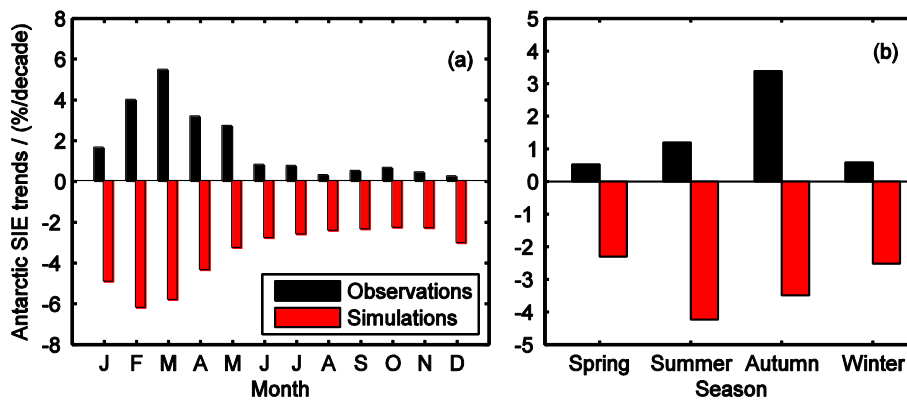
444 **Figures**



445

446 Figure 1. Climatology (a), anomaly and linear trend (b) of satellite observed and
 447 CMIP5 simulated Antarctic sea ice extent during 1979-2005. Two annual cycles are
 448 plotted in (a). The error bar is the range of one standard deviation.

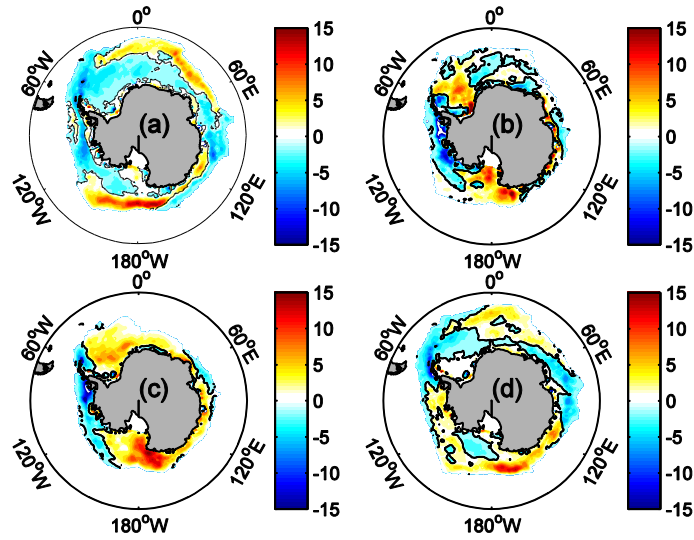
449



450

451 Figure 2. Monthly (a) and seasonal (b) linear trends of satellite observed and
 452 CMIP5-simulated Antarctic sea ice extent during 1979-2005.

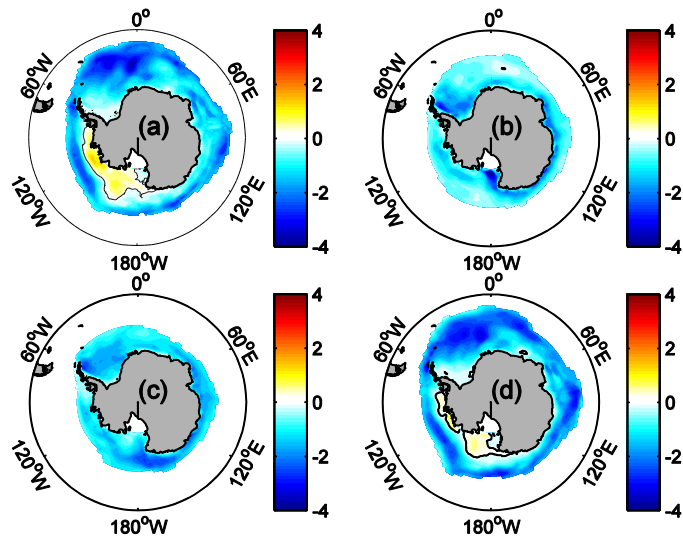
453



454

455 Figure 3. Linear trends (unit: % per decade) of satellite observed Antarctic sea ice
 456 concentration during 1979 to 2005. (a) Spring, (b) summer, (c) autumn, and (d)
 457 winter.

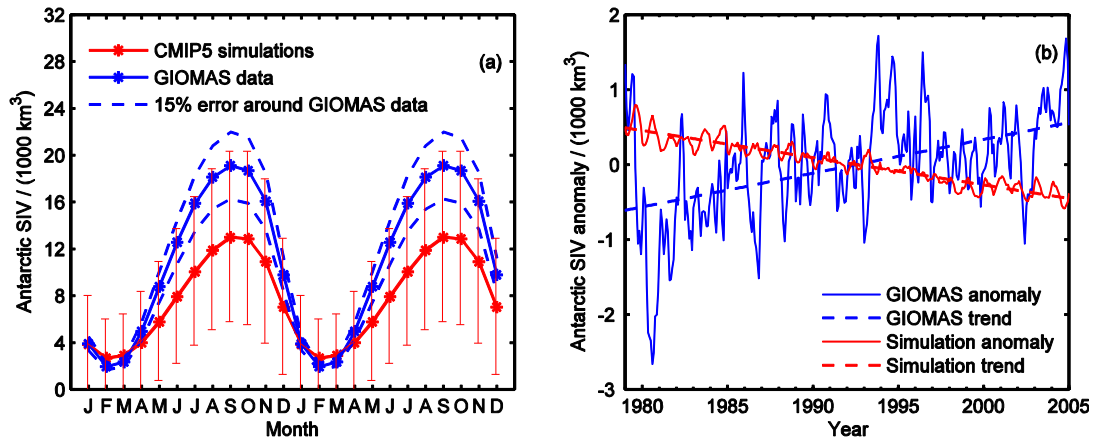
458



459

460 Figure 4. Linear trends (units: % per decade) of CMIP5-simulated Antarctic sea ice
 461 concentration during 1979-2005. (a) Spring, (b) summer, (c) autumn, and (d) winter.

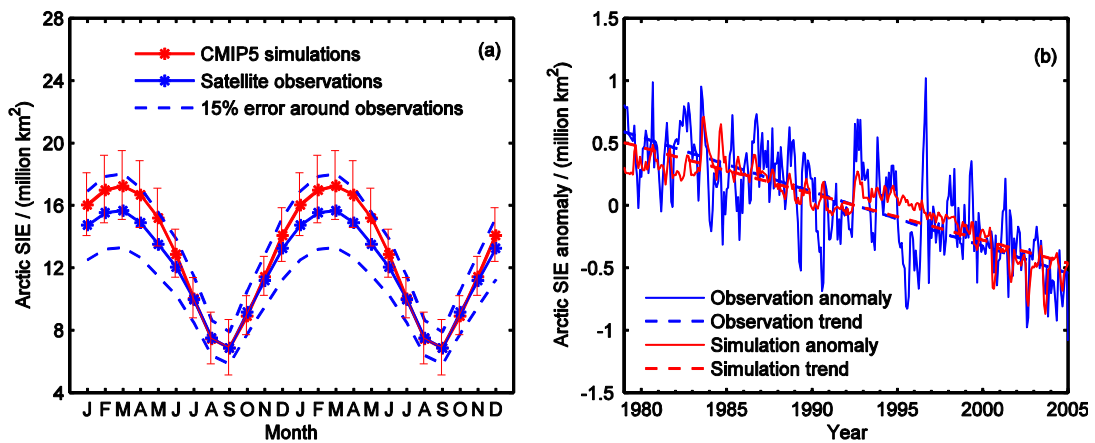
462



463

464 Figure 5. Climatology (a), anomaly and linear trend (b) of GIOMAS and CMIP5
 465 simulated Antarctic sea ice volume during 1979-2005. Two annual cycles are plotted
 466 in (a). The error bar is the range of one standard deviation.

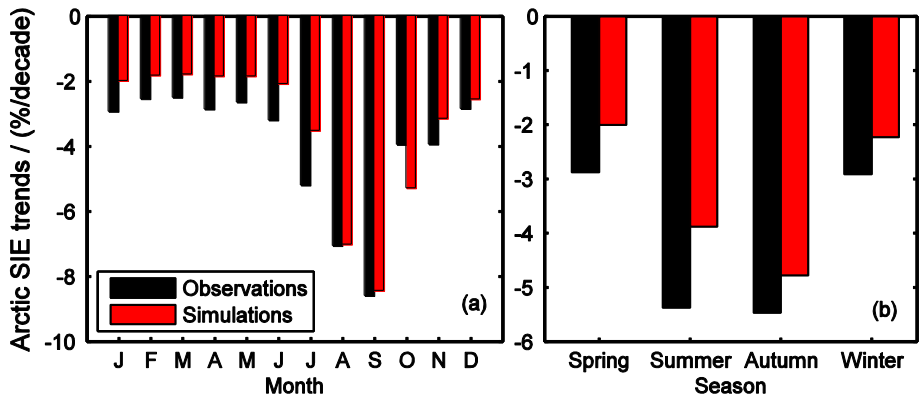
467



468

469 Figure 6. Climatology (a), anomaly and linear trend (b) of satellite observed and
 470 CMIP5-simulated Arctic sea ice extent during 1979-2005. Two annual cycles are
 471 plotted in (a). The error bar is the range of one standard deviation.

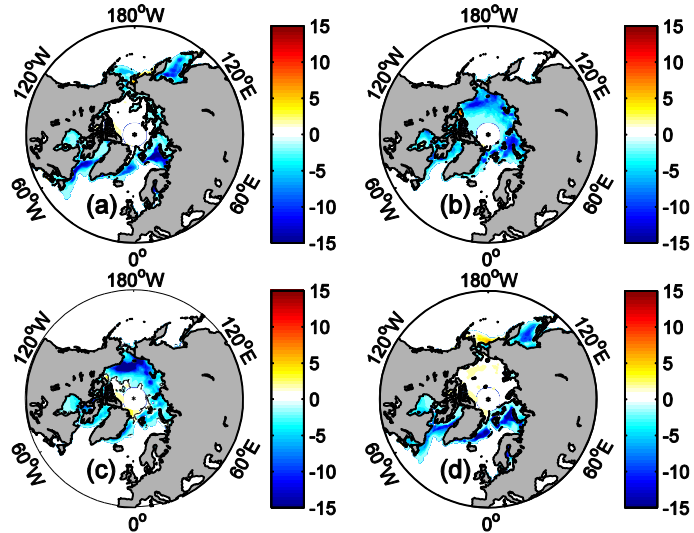
472



473

474 Figure 7. Monthly (a) and seasonal (b) linear trends of satellite observed and
 475 CMIP5-simulated Arctic sea ice extent during 1979-2005.

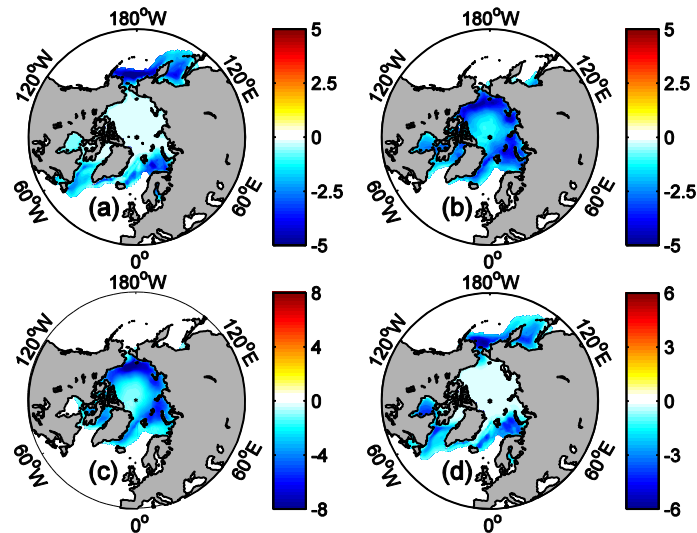
476



477

478 Figure 8. Linear trends (units: % per decade) of satellite observed Arctic sea ice
 479 concentration during 1979-2005. (a) Spring, (b) summer, (c) autumn, and (d) winter.

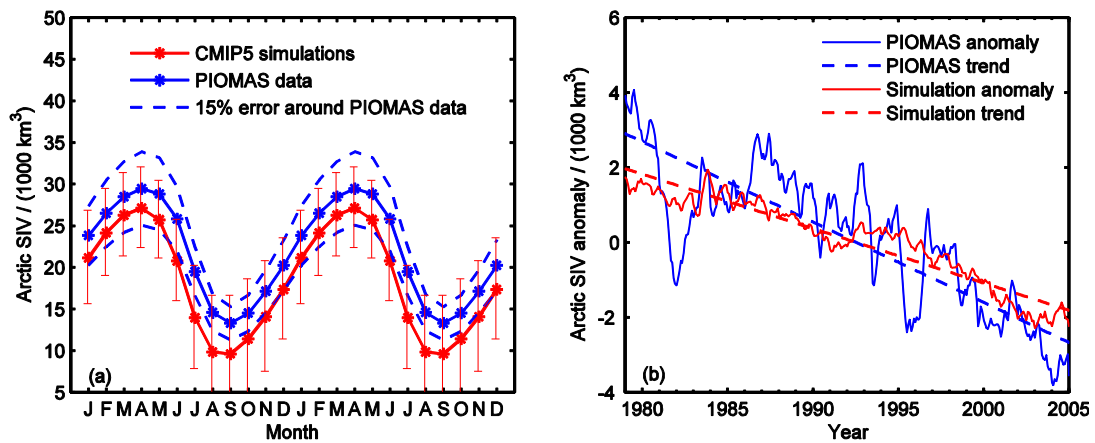
480



481

482 Figure 9. Linear trends (units: % per decade) of CMIP5-simulated Arctic sea ice
 483 concentration during 1979-2005. (a) Spring, (b) summer, (c) autumn, and (d) winter.

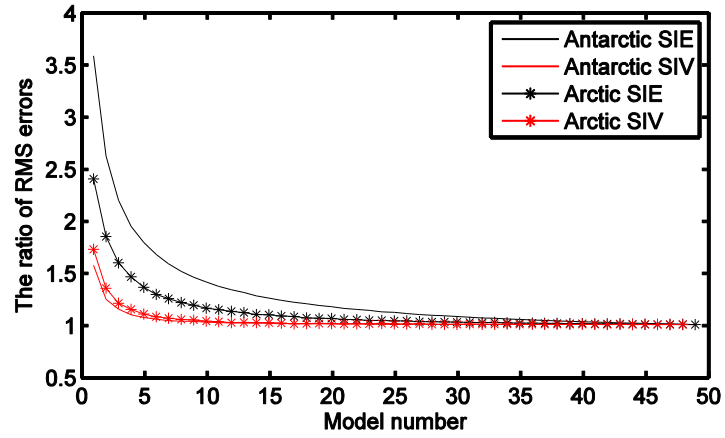
484



485

486 Figure 10. Climatology (a), anomaly and linear trend (b) of PIOMAS and
 487 CMIP5-simulated Arctic sea ice volume during 1979-2005. Two annual cycles are
 488 plotted in (a). The error bar is the range of one standard deviation.

489



490

491 Figure 11. The ratio of SIE and SIV RMS errors between the errors calculated using
492 different number of CMIP5 models and the error calculated using all 49 CMIP5
493 models.

494

495 **Tables**

496 Table 1. Antarctic sea ice metrics in CMIP5 models, satellite observations and GIOMAS dataset. Column (a) is mean annual SIE in million km².
 497 Column (b) is monthly SIE amplitude in million km². Column (c) is standard deviation of detrended monthly SIE anomaly in million km².
 498 Column (d) is linear trend in monthly SIE in 10⁵ km² decade⁻¹, and the value in parentheses is 95% confidence level. Column (e) is monthly SIE
 499 root mean square error in million km². Column (f) is mean annual SIV in 10³ km³. Column (g) is monthly SIV amplitude in 10³ km³. Column (h)
 500 is standard deviation of detrended monthly SIV anomaly in 10³ km³. Column (i) is linear trend in monthly SIV in 10³ km³ decade⁻¹, and the
 501 value in parentheses is 95% confidence level. Column (j) is monthly SIV root mean square error in 10³ km³.

Data sources or CMIP5 models	(a)	(b)	(c)	(d)	(e)	(f)	(g)	(h)	(i)	(j)
Observations or GIOMAS	11.94	15.70	0.40	1.29(0.57)	----	11.02	17.17	0.63	0.45(0.09)	----
Multi-model ensemble mean (MME)	11.50	15.46	0.11	-3.36(0.15)	0.71	7.73	10.31	0.10	-0.36(0.01)	4.20
ACCESS1.0	12.10	19.12	0.59	-1.72(0.83)	1.57	6.30	11.35	0.43	-0.15(0.06)	5.20
ACCESS1.3	14.24	15.77	0.54	-0.97(0.77)	2.31	10.71	9.78	0.67	-0.03(0.09)	2.75
BCC-CSM1.1	13.42	19.32	1.27	2.71(1.78)	2.11	7.13	11.51	0.92	0.09(0.13)	4.41
BCC-CSM1-1-M	12.26	18.86	1.06	-20.03(1.49)	1.52	5.65	9.98	0.71	-1.20(0.10)	5.92
BNU-ESM	20.60	23.46	0.82	-9.60(1.15)	9.19	18.49	22.48	0.87	-2.03(0.12)	7.89
CanCM4	14.65	20.58	0.74	-2.79(1.03)	3.40	3.09	4.81	0.28	-0.06(0.04)	9.21
CanESM2	14.69	20.64	0.96	-7.74(1.35)	3.42	3.09	4.82	0.40	-0.15(0.06)	9.22

Data sources or CMIP5 models	(a)	(b)	(c)	(d)	(e)	(f)	(g)	(h)	(i)	(j)
CCSM4	18.37	13.70	0.58	-7.34(0.82)	6.64	19.34	18.63	1.12	-1.56(0.16)	8.34
CESM1-BGC	17.67	14.05	0.49	-6.68(0.69)	5.93	18.28	18.31	0.91	-1.19(0.13)	7.28
CESM1-CAM5	14.06	14.78	0.47	-5.52(0.66)	2.58	11.22	16.05	0.58	-0.97(0.08)	1.13
CESM1-CAM5-1-FV2	13.01	14.11	0.58	-3.16(0.82)	1.77	9.96	14.12	0.74	-0.22(0.10)	1.89
CESM1-FASTCHEM	17.86	13.42	0.60	-8.78(0.84)	6.14	18.41	18.15	1.18	-1.70(0.17)	7.42
CESM1-WACCM	14.33	12.57	0.39	-6.45(0.54)	2.95	11.55	13.15	0.66	-0.91(0.09)	1.80
CMCC-CESM	11.84	19.43	0.99	2.91(1.39)	2.01	6.70	11.18	0.71	0.26(0.10)	4.91
CMCC-CM	11.81	16.84	0.67	-2.49(0.94)	0.90	6.82	10.14	0.48	-0.05(0.07)	4.97
CMCC-CMS	11.74	19.33	0.87	-1.52(1.23)	1.83	6.31	10.70	0.59	-0.12(0.08)	5.34
CNRM-CM5	7.78	16.98	0.77	-2.59(1.09)	4.53	3.01	7.81	0.42	-0.10(0.06)	8.79
CNRM-CM5-2	9.28	14.08	1.08	4.29(1.51)	3.16	4.93	9.78	1.02	0.38(0.14)	6.77
CSIRO-Mk3.6	15.92	12.11	0.67	-1.64(0.95)	4.89	12.13	13.28	0.65	-0.29(0.09)	2.62
EC-EARTH	10.66	17.18	0.66	-7.94(0.92)	1.72	6.09	9.44	0.58	-0.66(0.08)	5.75
FGOALS-g2	17.10	17.29	0.48	-1.47(0.67)	5.28	15.65	13.89	0.74	-0.14(0.10)	4.88
FIO-ESM	17.19	12.21	0.49	-8.53(0.68)	5.61	21.23	13.98	1.16	-1.57(0.16)	10.31
GFDL-CM2p1	8.00	15.38	0.81	-6.33(1.14)	4.01	2.45	5.55	0.30	-0.19(0.04)	9.57
GFDL-CM3	6.25	12.06	0.73	-6.82(1.02)	5.82	1.92	4.16	0.37	-0.30(0.05)	10.29
GFDL-ESM2G	8.11	14.34	0.63	-4.45(0.88)	3.90	2.71	5.81	0.41	-0.24(0.06)	9.31
GFDL-ESM2M	6.39	12.23	0.41	-1.61(0.58)	5.65	1.81	4.20	0.16	-0.09(0.02)	10.36

Data sources or CMIP5 models	(a)	(b)	(c)	(d)	(e)	(f)	(g)	(h)	(i)	(j)
GISS-E2-H	6.21	10.62	0.38	-1.89(0.53)	6.03	3.24	7.19	0.27	-0.24(0.04)	8.65
GISS-E2-H-CC	12.18	19.07	0.75	-5.75(1.05)	1.52	6.70	14.16	0.51	-0.54(0.07)	4.57
GISS-E2-R	7.74	14.31	1.01	-3.39(1.42)	4.31	3.06	6.17	0.47	-0.16(0.07)	8.92
GISS-E2-R-CC	8.12	14.55	0.66	0.82(0.92)	3.93	3.12	6.24	0.35	0.00(0.05)	8.86
HadCM3	14.26	19.95	0.78	-2.74(1.10)	3.28	14.70	21.87	0.83	-0.49(0.12)	4.13
HadGEM2-AO	9.11	14.29	0.59	-5.31(0.83)	3.20	5.58	9.70	0.49	-0.42(0.07)	6.26
HadGEM2-CC	9.12	14.29	0.72	-0.85(1.02)	3.25	5.50	9.68	0.61	-0.05(0.09)	6.34
HadGEM2-ES	9.82	15.02	0.70	-3.25(0.98)	2.60	6.16	10.33	0.61	-0.41(0.09)	5.66
INMCM4	6.25	10.91	0.48	-4.00(0.68)	6.04	2.81	6.12	0.38	-0.28(0.05)	9.21
IPSL-CM5A-LR	9.66	19.06	0.84	-5.03(1.17)	3.43	4.13	8.66	0.53	-0.26(0.07)	7.70
IPSL-CM5A-MR	8.08	17.30	0.74	1.69(1.04)	4.56	2.80	6.50	0.35	0.01(0.05)	9.21
IPSL-CM5B-LR	3.34	8.09	0.42	0.59(0.59)	9.09	1.22	3.32	0.20	0.04(0.03)	11.10
MIROC4h	10.90	17.53	0.61	-7.96(0.86)	1.33	5.35	9.74	0.41	-0.51(0.06)	6.28
MIROC5	3.23	6.62	0.29	-1.03(0.41)	9.29	1.40	3.15	0.16	-0.07(0.02)	10.93
MIROC-ESM	12.65	19.12	0.64	-5.83(0.91)	1.47	7.23	10.72	0.47	-0.48(0.07)	4.46
MIROC-ESM-CHEM	13.38	19.80	0.53	-2.15(0.74)	2.07	8.08	11.59	0.49	-0.21(0.07)	3.61
MPI-ESM-LR	7.70	15.08	0.73	-2.95(1.03)	4.50	3.41	6.35	0.38	-0.19(0.05)	8.64
MPI-ESM-MR	7.90	15.62	0.84	4.41(1.17)	4.28	3.54	7.06	0.48	0.24(0.07)	8.39
MPI-ESM-P	7.91	15.69	0.75	-0.25(1.06)	4.34	3.48	6.48	0.45	0.05(0.06)	8.56

Data sources or CMIP5 models	(a)	(b)	(c)	(d)	(e)	(f)	(g)	(h)	(i)	(j)
MRI-CGCM3	13.43	15.99	0.66	1.52(0.93)	1.67	10.72	13.05	0.63	0.22(0.09)	2.04
MRI-ESM1	13.24	16.32	0.75	-0.62(1.05)	1.53	10.14	13.00	0.58	-0.03(0.08)	2.25
NorESM1-M	13.08	14.19	0.57	-0.71(0.80)	1.24	13.88	12.41	1.17	-0.07(0.16)	3.66
NorESM1-ME	16.98	14.19	0.60	-3.77(0.84)	5.24	17.57	16.82	1.40	-0.74(0.20)	6.59

502

503 Table 2. Arctic sea ice metrics in CMIP5 models, satellite observations and PIOMAS dataset. Column (a) is mean annual SIE in million km².
504 Column (b) is monthly SIE amplitude in million km². Column (c) is standard deviation of detrended monthly SIE anomaly in million km².
505 Column (d) is linear trend in monthly SIE in 10⁵ km² decade⁻¹, and the value in parentheses is 95% confidence level. Column (e) is monthly SIE
506 root mean square error in million km². Column (f) is mean annual SIV in 10³ km³. Column (g) is monthly SIV amplitude in 10³ km³. Column (h)
507 is standard deviation of detrended monthly SIV anomaly in 10³ km³. Column (i) is linear trend in monthly SIV in 10³ km³ decade⁻¹, , and the
508 value in parentheses is 95% confidence level. Column (j) is monthly SIV root mean square error in 10³ km³.

Data sources or CMIP5 models	(a)	(b)	(c)	(d)	(e)	(f)	(g)	(h)	(i)	(j)
Observations or PIOMAS	12.02	8.80	0.29	-4.35(0.41)	----	21.85	16.17	1.02	-2.14(0.14)	----
Multi-model ensemble mean (MME)	12.81	10.40	0.13	-3.71(0.19)	1.07	18.45	17.50	0.35	-1.45(0.05)	3.57
ACCESS1.0	12.13	10.33	0.41	-5.51(0.57)	0.94	15.41	18.74	1.05	-1.58(0.15)	6.60
ACCESS1.3	11.79	9.47	0.43	-0.78(0.60)	0.73	18.81	17.02	1.02	-1.05(0.14)	3.23

Data sources or CMIP5 models	(a)	(b)	(c)	(d)	(e)	(f)	(g)	(h)	(i)	(j)
BCC-CSM1.1	14.86	15.39	0.69	-8.79(0.97)	3.70	14.29	22.70	1.00	-2.01(0.14)	8.02
BCC-CSM1-1-M	13.19	15.96	0.65	-5.19(0.92)	2.87	11.04	20.69	0.87	-0.74(0.12)	11.02
BNU-ESM	14.72	12.61	0.50	-4.41(0.70)	3.19	23.03	19.79	1.23	-4.37(0.17)	1.83
CanCM4	12.79	14.77	0.52	-4.97(0.73)	2.49	11.41	15.35	0.97	-0.38(0.14)	10.47
CanESM2	12.01	13.76	0.49	-6.80(0.69)	1.91	9.97	14.21	0.63	-1.18(0.09)	11.92
CCSM4	12.33	8.56	0.44	-1.34(0.62)	0.42	20.27	16.16	1.51	-1.54(0.21)	1.82
CESM1-BGC	12.10	7.96	0.41	-2.85(0.58)	0.35	20.30	15.52	1.51	-2.63(0.21)	1.86
CESM1-CAM5	12.33	8.35	0.38	-1.87(0.53)	0.52	22.73	16.01	1.96	-1.22(0.28)	1.35
CESM1-CAM5-1-FV2	12.52	8.68	0.42	-5.07(0.59)	0.64	23.17	16.01	1.87	-3.63(0.26)	1.49
CESM1-FASTCHEM	12.02	8.86	0.39	-3.70(0.55)	0.25	18.27	15.86	1.37	-1.98(0.19)	3.69
CESM1-WACCM	13.44	8.10	0.36	-2.88(0.51)	1.51	27.32	9.47	2.07	0.09(0.29)	6.27
CMCC-CESM	13.97	9.33	0.36	-2.63(0.51)	2.12	28.75	11.93	1.38	-1.44(0.19)	7.11
CMCC-CM	13.99	7.35	0.30	-5.09(0.43)	2.06	33.01	9.87	1.73	-2.40(0.24)	11.52
CMCC-CMS	12.64	7.92	0.34	-2.87(0.48)	0.82	28.29	9.73	1.29	-1.18(0.18)	6.89
CNRM-CM5	12.41	11.41	0.46	-7.58(0.65)	1.11	14.44	20.22	0.99	-1.76(0.14)	7.60
CNRM-CM5-2	14.20	10.65	0.45	-2.32(0.63)	2.40	20.11	21.83	1.29	-0.96(0.18)	2.76
CSIRO-Mk3.6	16.13	7.57	0.30	-5.33(0.42)	4.20	25.94	12.16	0.81	-2.32(0.11)	4.30
EC-EARTH	12.45	8.04	0.35	-3.84(0.49)	0.57	24.01	12.44	1.90	-0.59(0.27)	2.86
FGOALS-g2	11.68	3.35	0.13	-1.44(0.18)	1.86	-----	----	----	----	----

Data sources or CMIP5 models	(a)	(b)	(c)	(d)	(e)	(f)	(g)	(h)	(i)	(j)
FIO-ESM	12.46	10.27	0.40	-2.23(0.57)	1.00	18.94	18.96	1.86	-1.69(0.26)	3.15
GFDL-CM2p1	12.58	12.85	0.54	-3.76(0.75)	1.68	11.11	18.13	0.87	-1.01(0.12)	10.80
GFDL-CM3	12.22	8.71	0.33	-2.89(0.46)	0.41	15.25	15.47	1.31	-1.18(0.18)	6.61
GFDL-ESM2G	15.72	13.72	0.48	-7.05(0.68)	4.24	16.91	19.33	1.24	-1.77(0.17)	5.17
GFDL-ESM2M	12.46	11.06	0.53	-0.31(0.74)	0.98	12.13	16.11	1.02	-0.56(0.14)	9.75
GISS-E2-H	12.96	14.87	0.54	-5.07(0.75)	2.47	13.61	25.67	0.76	-0.91(0.11)	9.10
GISS-E2-H-CC	13.94	14.24	0.60	-5.91(0.84)	2.80	14.94	27.49	0.80	-1.29(0.11)	8.23
GISS-E2-R	13.65	15.17	0.49	-6.31(0.69)	2.89	15.50	29.32	0.75	-1.28(0.11)	8.17
GISS-E2-R-CC	15.13	16.73	0.48	-5.65(0.67)	4.28	17.16	31.86	0.76	-1.08(0.11)	7.64
HadCM3	13.94	13.59	0.56	-4.74(0.78)	2.78	21.07	26.96	0.87	-2.25(0.12)	4.46
HadGEM2-AO	11.38	10.75	0.40	-3.81(0.56)	1.15	16.58	20.16	0.84	-0.98(0.12)	5.53
HadGEM2-CC	13.20	10.68	0.45	-3.10(0.63)	1.45	21.56	21.55	0.96	-2.47(0.13)	2.22
HadGEM2-ES	12.34	11.21	0.43	-6.03(0.60)	1.14	18.85	21.13	1.00	-1.69(0.14)	3.64
INMCM4	12.92	12.02	0.42	-0.21(0.59)	1.61	15.20	22.08	0.96	-0.21(0.13)	7.07
IPSL-CM5A-LR	12.72	10.07	0.44	-3.03(0.62)	1.14	21.87	16.41	1.48	-0.96(0.21)	1.66
IPSL-CM5A-MR	11.06	9.55	0.35	-2.85(0.49)	1.25	14.83	16.32	0.92	-1.69(0.13)	7.17
IPSL-CM5B-LR	14.06	8.28	0.40	-0.77(0.56)	2.08	27.28	13.11	2.91	-1.37(0.41)	6.25
MIROC4h	10.66	9.65	0.40	-3.11(0.56)	1.47	10.86	16.48	0.82	-1.00(0.12)	11.02
MIROC5	12.12	6.63	0.29	-6.78(0.40)	0.65	25.31	14.88	1.09	-3.68(0.15)	3.81

Data sources or CMIP5 models	(a)	(b)	(c)	(d)	(e)	(f)	(g)	(h)	(i)	(j)
MIROC-ESM	10.40	8.05	0.34	-1.91(0.47)	1.69	11.09	14.36	0.62	-1.04(0.09)	10.79
MIROC-ESM-CHEM	10.83	7.89	0.46	-4.24(0.65)	1.30	12.59	14.73	1.39	-1.69(0.20)	9.29
MPI-ESM-LR	11.10	7.95	0.40	-2.48(0.56)	1.01	15.07	16.87	0.85	-1.23(0.12)	6.85
MPI-ESM-MR	11.07	8.00	0.40	-4.94(0.56)	1.02	15.20	17.30	0.90	-1.75(0.13)	6.74
MPI-ESM-P	10.94	8.27	0.34	-1.83(0.48)	1.13	13.45	17.05	1.13	-0.80(0.16)	8.46
MRI-CGCM3	15.01	15.27	0.47	-1.44(0.66)	3.97	15.70	19.40	1.48	-0.55(0.21)	6.33
MRI-ESM1	14.65	14.67	0.61	-4.07(0.86)	3.52	15.21	18.89	1.74	-1.56(0.24)	6.76
NorESM1-M	12.01	5.96	0.25	-1.98(0.36)	0.90	23.77	11.23	1.57	-0.68(0.22)	3.11
NorESM1-ME	12.47	5.99	0.31	-0.21(0.43)	0.97	23.97	9.71	2.14	-0.46(0.30)	3.69